Journal of Alloys and Compounds 509 (2011) 3832–3836

Contents lists available at ScienceDirect

Journal of Alloys and Compounds

journal homepage: www.elsevier.com/locate/jallcom

Optical and microhardness studies on unidirectional grown triaqua glycine sulfato zinc (II): A semiorganic NLO crystal

J. Mary Linet*, S. Dinakaran, S. Jerome Das

Department of Physics, Loyola College, Chennai 600034, India

ARTICLE INFO

Article history:
Received 17 September 2010
Received in revised form 9 December 2010
Accepted 10 December 2010
Available online 21 December 2010

Keywords:
Optical materials
Crystal growth
Optical properties
Nonlinear optics

ABSTRACT

Good optical quality bulk single crystal of triaqua glycine sulfato zinc (II) has been grown by unidirectional crystal growth method. The crystal of 76 mm length and 12 mm diameter has been obtained at an average growth rate of 3.5 mm/day. The grown crystal was identified by single crystal X-ray analysis and the functional groups present in the crystal lattice were confirmed by Fourier transform infrared spectral analysis. The crystalline perfection of the grown crystal was determined through high resolution X-ray analysis. The transmission spectral analysis shows more than 80% of transmission in the entire visible region which exhibits the good optical quality of the grown crystal and the second harmonic generation efficiency was identified by Kurtz powder test. The mechanical strength of the grown crystal was studied and the results are discussed in detail.

1. Introduction

In recent years there has been considerable interest to synthesize semiorganic nonlinear optical materials with excellent second order optical non linearities owing to their potential application in electro-optic and opto-electronics devices [1]. Metal–organic coordination compounds have attracted attention for their considerable high NLO coefficients, stable physico-chemical properties and better mechanical intension such as zinc tris (thiourea) sulfate [2,3] and bis thiourea cadmium chloride [4]. Since several decades, efforts have been made to grow amino acid mixed inorganic complex crystals, in order to improve the mechanical and thermal stability. A series of amino acid based complex semiorganic compounds such as L-arginine phosphate [5], L-histidine bromide [6], L-arginine hydrochloride monohydrate [7], L-arginine trifluoroacetate [8], and glycinium phosphate [9], have been grown and reported to have improved mechanical and thermal stabilities by the presence of inorganic compounds. Glycine [NH_2CH_2COOH] is the simplest amino acid, it crystallizes in three kinds of polymorphs such as α, β and γ, which exhibit different physical properties. As both α and β glycine crystallize in the centrosymmetric space group $P2_1/n$, it is impossible to generate second harmonic generation, while gamma glycine posses non centro symmetric space group $P3_1$ and it exhibits NLO property [10]. Recent literature reports show that glycine combines with inorganic materials like $LiSO_4$ [11], $LiCl_2$ [12], $ZnCl_2$ [13] and $NaNO_2$ [14] and these crystallize in the noncentrosymmetric space group and are identified as non-linear optical materials. These molecular organic crystals are exceptionally interesting for non-linear optics and different kinds of photo induced changes due to the large difference between the intramolecular and inter-molecular chemical bonds. This may lead to the occurrence of a large number of molecular defect levels within the energy band [15]. Triaqua glycine sulfato zinc (II) (TGSZ) is a semiorganic NLO crystal which crystallizes in the orthorhombic system with space group $Pca2_1$ and lattice parameters $a = 8.440$ Å, $b = 8.278$ Å, $c = 12.521$ Å [16]. In the present investigation, solubility and metastable zone width measurements have been carried out at different temperatures and the obtained data was used to grow the bulk single crystal of TGSZ along <0 0 1> direction by unidirectional crystal growth method for the first time. The grown crystal has been subjected to single crystal XRD analysis, FTIR, high resolution X-ray analysis, optical transmission spectral analysis, Kurtz powder test and microhardness studies.

2. Experimental details

2.1. Synthesis of TGSZ

Analytical grade glycine and zinc sulfate heptahydrate taken in equimolar ratio was used to synthesize triaqua glycine sulfato zinc (II). The chemical reaction of the synthesis is as follows:

$$CH_2NH_2COOH + ZnSO_4{\cdot}7H_2O \rightarrow [Zn(H_2O)_3(CH_2NH_3{}^+COO^-)(SO_4)] + 4H_2O \quad (1)$$

The synthesized salt prepared from the above chemical reaction was further purified by repeated crystallization.

* Corresponding author. Tel.: +91 44 2817 5662; fax: +91 44 2817 5566.
E-mail address: linet.mary@gmail.com (J. Mary Linet).

0925-8388/$ – see front matter © 2010 Elsevier B.V. All rights reserved.
doi:10.1016/j.jallcom.2010.12.083

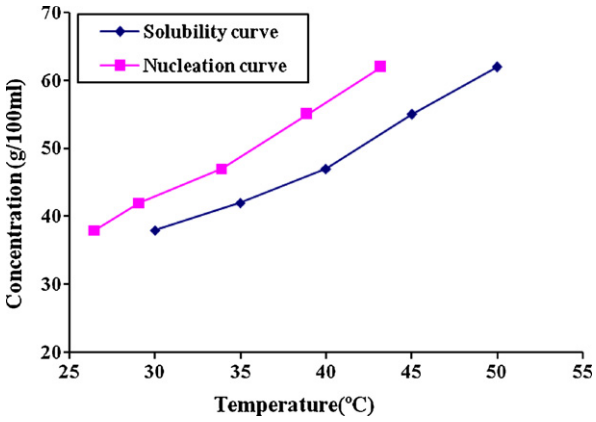

Fig. 1. Solubility and nucleation curve of TGSZ.

2.2. Solubility and metastable zone width measurement

Solubility studies were carried out using synthesized salt of TGSZ and double distilled water. The solution was kept in a constant temperature bath maintained at 30 °C (accuracy ±0.1 °C) and continuously stirred using motorized magnetic stirrer, to have uniform temperature and concentration throughout the volume of the solution. After attaining supersaturation, the equilibrium concentration of the solute was analyzed gravimetrically [17]. The same procedure was repeated for temperatures from 35 °C to 50 °C with 5 °C interval. The nucleation studies were carried out in a constant temperature bath controlled to an accuracy of ±0.05 °C, provided with a cryostat. A constant volume of 100 ml solution was used for all experiments. The solution was preheated to 5 °C above the saturation temperature, 1 h before cooling and continuously stirred to ensure homogeneous concentration and temperature through the entire volume (100 ml) of the solution. The metastable zone width was measured by polythermal method [18]. In this method, the saturated equilibrium solution was cooled from the preheated temperature to the nucleation temperature where the first visible nucleus called the critical nucleus is identified. The solubility and nucleation curve is shown in Fig. 1. The solubility curve shows positive solubility gradient and nucleation curve exhibits that the metastable zone width is low at 30 °C (~4 °C) and the width increases with temperature (7 °C at 50 °C).

2.3. Solution preparation

Saturated solution was prepared at 45 °C according to the solubility data. The calculated amount of glycine and zinc sulfate heptahydrate was dissolved in double distilled water to prepare the saturated solution. Prepared solution was over heated by 10 °C above the saturation point to avoid spontaneous nucleation during filtration. Whatman filter paper of porosity 2.5 μm was used to filter the solution.

2.4. Crystal growth

Crystal growth was adopted using unidirectional crystal growth method reported by Sankaranarayan and Ramasamy [19]. This technique offers the main benefit of growing a crystal along a specific orientation instead of natural facets. It results in reducing the wasteful portion of the crystal for device applications and the high percentage of solute–solvent conversion efficiency [20]. The detail description of the crystal growth setup is reported elsewhere [21]. Spontaneously obtained good quality crystal was used as seed. The seed was reshaped to conical shape to fix at the bottom of the ampoule along <0 0 1> direction parallel to the vertical axis of the ampoule. Seed fixed ampoule was immersed in the crystal growth setup at room temperature. To avoid the thermal stress on seed crystal the temperature of the bath was gradually increased. Then the saturated solution was filled in the ampoule for growth. The temperatures of the top and bottom portion were chosen according to the solubility and nucleation curve, which helps to avoid spurious nucleation during growth. At 45 °C, the metastable zone width was found to be high of about ~7 °C. Therefore, in the present experiment we have used $\Delta T = 4$ °C between the top and bottom portion. For the complete duration of the growth run, the temperature at the top and bottom of the ampoule was maintained as 44 °C and 40 °C respectively which helps to create a thermal gradient inside the growth apparatus. Due to the action of gravity, the concentration gradient is shifted towards the seed crystal which helps in the growth and the slow evaporation results in the increase in the density of the solution at top which induces buoyancy convection which further helps in increasing the concentration towards the growing crystal. A crystal of length 75 mm and 12 mm diameter was grown in a period of 22 days with an average growth rate of 3.5 mm per day. The photograph of as grown crystal of TGSZ is shown in Fig. 2.

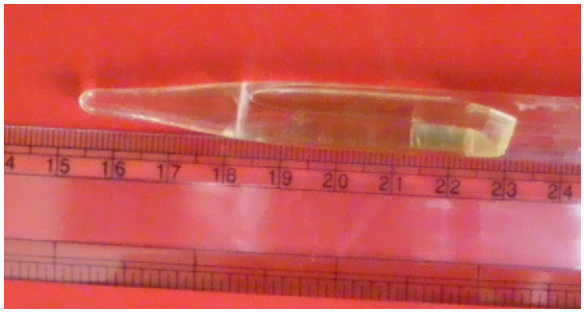

Fig. 2. Grown crystal of TGSZ.

3. Results and discussion

3.1. Single crystal X-ray analysis

The single crystal data of the grown crystal was carried out using Bruker Kappa APEX-2 diffractometer with Mo Kα (λ = 0.7103 Å). The results show that the crystal belongs to the orthorhombic system with point group and space group, *mm*2 and $Pca2_1$ respectively. The calculated lattice parameters were $a = 8.445$ Å, $b = 8.279$ Å, $c = 12.530$ Å which are in good agreement with the literature report [16].

3.2. FTIR spectral analysis

Functional groups present in the crystal were confirmed by FTIR analysis using Bruker IFS-66v between the range of 4000 and 400 cm^{-1}. The FTIR spectrum of the grown crystal is shown in Fig. 3. The peak at 3420 cm^{-1} is due to OH stretch of water. The peak at 3206 cm^{-1} is due to NH_3^+ asymmetric stretching. C=O asymmetric stretching is observed at 1642 cm^{-1}. The CH_2 bending is observed at 1496 cm^{-1}. C=O symmetric stretching is observed at 1412 cm^{-1}. The peaks at 1104 cm^{-1} and 618 cm^{-1} indicate the presence of S–O stretching. The peak observed at 1318 cm^{-1} is due to the CH_2 wagging vibrations. The CH out of plane bending and out of plane deformation is observed at 983 cm^{-1} and 904 cm^{-1} respectively. The peak at 748 cm^{-1} is due to OH deformation.

3.3. High resolution X-ray diffractometry

The crystalline perfection of the grown single crystals was characterized by high resolution X-ray analysis (HRXRD) by employing a multicrystal X-ray diffractometer developed at NPL [22]. The well-

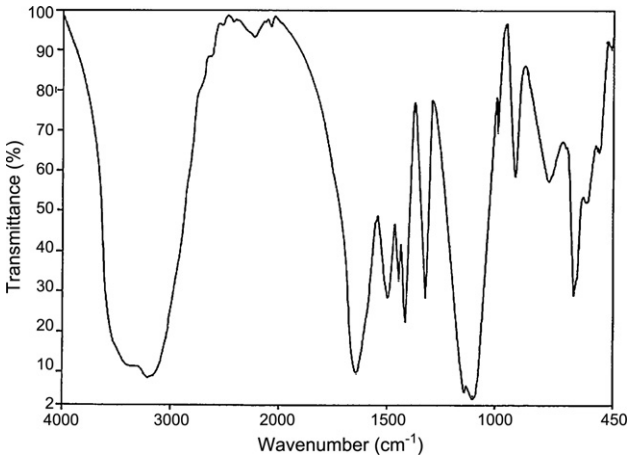

Fig. 3. FTIR spectrum of TGSZ.

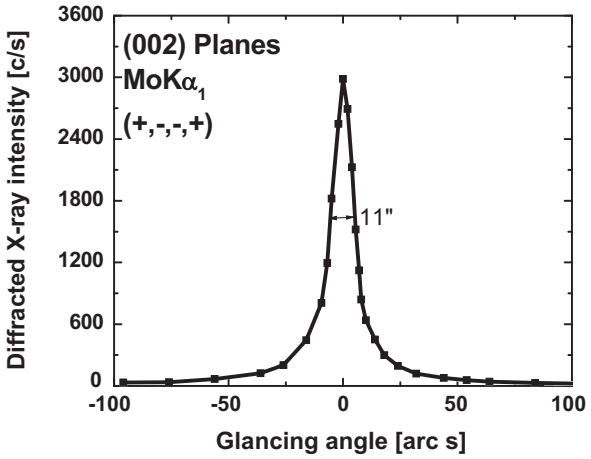

Fig. 4. High resolution X-ray diffraction curve recorded for TGSZ single crystal.

collimated and monochromated Mo $K\alpha_1$ beam obtained from the three monochromator Si crystals set in dispersive (+,−,−) configuration has been used as the exploring X-ray beam. The specimen crystal was aligned in the (+,−,−,+) configuration. Due to dispersive configuration, though the lattice constants of the monochromator crystal(s) and the specimen were different, the unwanted dispersion broadening in the diffraction curve (DC) of the specimen crystal is insignificant. Fig. 4 shows the high-resolution diffraction curve (DC) recorded for TGSZ specimen using (0 0 2) diffracting planes in symmetrical Bragg geometry. As seen in the figure, the DC is quite sharp without any satellite peak which shows that the crystal has no internal structural grain boundaries [23]. The full width at half maximum (FWHM) of the diffraction curve is 11 arc sec, which is very close to that expected from the plane wave theory of dynamical X-ray diffraction [24]. The single sharp diffraction curve with very low FWHM indicates that the crystalline perfection is extremely good. The specimen is a nearly perfect single crystal without having any internal structural grain boundaries.

3.4. Transmission analysis

The transmission spectrum was recorded in the wavelength range between 200 nm and 1100 nm using Varian Cary 5E spectrophotometer. Several crystal plates from different portions of the crystal were subjected to transmission studies and all the plates showed ~80–88% of transmission in the entire visible and near-IR region which exhibits the good optical quality and homogeneity of the grown crystal. The absorption edge is found to be at 240 nm which exhibits that the crystal is also transparent in the blue region. Due to the high transmittance in the visible and blue region, TGSZ could be used as a potential candidate for NLO applications. Fig. 5 shows the transmission spectrum of TGSZ.

3.5. Second harmonic generation

The NLO conversion efficiency was tested using a modified setup of Kurtz and Perry [25]. A Q-switched Nd:YAG laser beam of wavelength 1064 nm was used with an input power of 2.0 mJ and pulse width of 10 ns at a repetition rate of 10 Hz. A small portion of TGSZ was powdered to a uniform particle size of about 125–150 mm and then packed in a capillary of uniform bore and exposed to laser radiations. The output from the sample was monochromated to collect only the second harmonic (532 nm) and the intensity was measured using a photomultiplier tube. A second harmonic signal of 95 mV was obtained, while the standard potassium dihydrogen phosphate (KDP) crystal gave an SHG signal of 45 mV/pulse for the same input energy. From the obtained results it was evident that the relative SHG efficiency of TGSZ was 2.1 times that of well known KDP crystal.

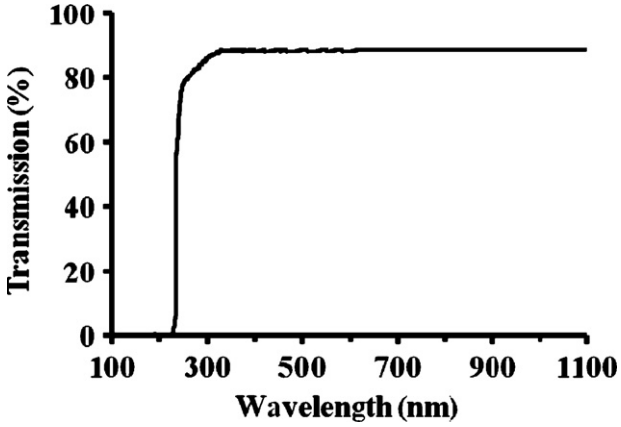

Fig. 5. Optical absorbance spectrum of TGSZ.

3.6. Microhardness studies

The mechanical strength of the grown crystal was studied using LEITZ WETZLER Vickers pyramidal indentor. Microhardness measurement is commonly used to determine the mechanical strength of the material which is related to bond strength and defect structure [26]. Optically clear and defect free crystal plate taken perpendicular to the growth direction was subjected to indentation tests at room temperature. The diagonal length of the indentation (d) in μm for various applied load (P) in g was measured for a constant indentation period of 15 s. The Vickers's hardness number (H_v) was calculated using the relation:

$$H_v = 1854.4\frac{P}{d^2}\ \text{kg/mm}^2 \quad (2)$$

The variation of H_v with the applied load P is shown in Fig. 6. According to the indentation size effect (ISE), microhardness of crystals decreases with increasing load and in reverse indentation size effect (RISE) hardness increases with increasing load. In our case, H_v increases with load up to 200 g and becomes load independent for $P \geq 200$ g. Similar observation is observed in alkaline earth nitrate crystals [26]. The traditional Meyer's law gives the relationship between load P and size d [27]:

$$P = Ad^n \quad (3)$$

where the exponent n is the Meyer's number and A is a constant. For normal ISE behaviour the exponent $n < 2$, when $n > 2$ there is

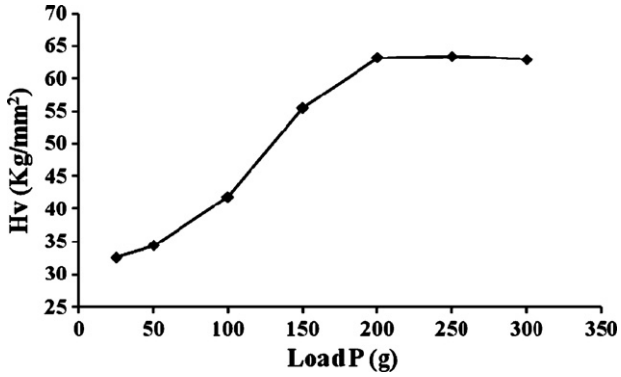

Fig. 6. Variation of H_v with applied load P.

Table 1
Hardness parameters of TGSZ.

Meyer index number (n)		Hardness, H_v (kg/mm^2)	W (g)	A_1 (g/μm^2)	Corrected hardness, H_0 (kg/mm^2)	Yield strength (MPa)
Low loads	High loads					
2.723	1.977	63	−47.61	0.039	72	235

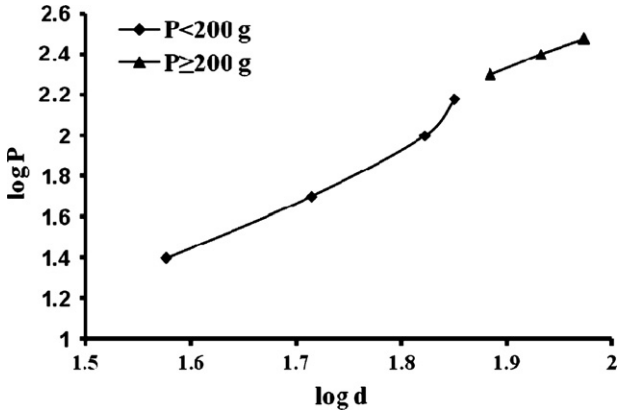

Fig. 7. Plot of log P vs. log d.

reverse ISE behaviour and when $n = 2$ the hardness is independent of applied load, which is given by Kick's law. Fig. 7 shows a plot of log P vs. log d for the grown crystal and is presented by two segments of plot for $P < 200$ g and $P \geq 200$ g. The estimated values of n are shown in Table 1.

According to Onistch, for hard materials n lies between 1 and 1.6 and for soft material it is above 1.6 [28]. So the value of n in Table 1 implies that TGSZ is a soft crystal.

According to Hays–Kendall's approach, load dependent hardness may be expressed by [29]:

$$P = W + A_1 d^n \tag{4}$$

where W is the minimum load initiate plastic deformation, A_1 is the load independent constant and the exponent $n = 2$. The value of W and A_1 can be calculated by plotting the experimental P against d^2. These two values have been estimated from the plot drawn between P and d^2 shown in Fig. 8. The corrected hardness H_0 has been estimated using the relation:

$$H_0 = 1854.4 \times A_1 \tag{5}$$

From the hardness value, the yield strength (σ_v) of the material can be found out using the relation:

$$\sigma_v = \frac{H_v}{2.9}[1 - (n-2)]\left[\frac{12.5(n-2)}{1-(n-2)}\right]^{n-2} \tag{6}$$

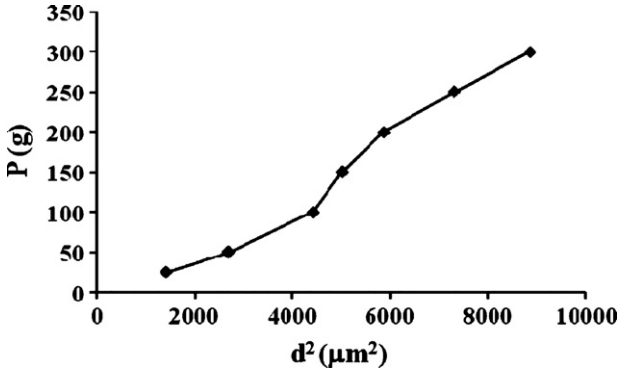

Fig. 8. Plot of load P vs. d^2.

for Meyer's index $n > 2$ and for $n \leq 2$ the above equation is reduced to:

$$\sigma_v = \frac{H_v}{3} \tag{7}$$

In the present case, the Meyer's index was found to be 1.977 and hence Eq. (7) was used to estimate the yield strength. The calculated hardness parameters are given in Table 1.

4. Conclusions

Optical quality bulk single crystal of triaqua glycine sulfato zinc (II) has been grown by unidirectional crystal growth technique from aqueous solution and an enhanced size of 76 mm length and 12 mm diameter crystal has been obtained with an average growth rate of 3.5 mm/day. Single crystal XRD analysis shows that the crystal belongs to the orthorhombic system with space group $Pca2_1$ and lattice parameters were found to be $a = 8.445$ Å, $b = 8.279$ Å, $c = 12.530$ Å. The functional groups present in the crystal lattice were confirmed by Fourier transform infrared spectral analysis. High-resolution X-ray analysis study resulted in a single sharp peak which shows no internal grain boundaries in the crystal and a rocking curve width of FWHM of 11 arc sec exhibits the good crystalline quality of the grown crystal. Transmission spectral analysis shows more than 80% of transmission in the entire visible region which exhibits the good optical quality of the grown crystal. The SHG efficiency of the grown crystal was found to be 2.1 times more than commercially available KDP crystal. The load variation of hardness has been explained on the basis of reverse indentation size effect and the Vickers hardness value was found to be 72 kg/mm^2.

Acknowledgements

The authors are grateful to SAIF, IIT Madras for characterization studies and the authors are grateful to Dr. G. Bhagavannarayanna, NPL, India for HRXRD studies.

References

[1] J. Thomas Joseph Prakash, S. Kumararaman, Mater. Lett. 62 (2008) 4003–4005.
[2] S. Verma, M.K. Singh, V.K. Wadhawan, C.H. Suresh, Pramana-J. Phys. 54 (6) (2000) 879–888.
[3] S. Dinakaran, S. Verma, S. Jerome Das, S. Kar, K.S. Bartwal, Cryst. Res. Technol. 45 (2010) 233–238.
[4] N.R. Dhumane, S.S. Hussaini, V.G. Dongre, P.P. Karmuse, M.D. Shirsat, Cryst. Res. Technol. 44 (2009) 269–274.
[5] S. Arjunan, A. Bhaskaran, R. Mohan Kumar, R. Mohan, R. Jayavel, J. Alloys Compd. 506 (2010) 784–787.
[6] N. Vijayan, G. Bhagavannarayana, K. Nagarajan, V. Upadhyaya, Mater. Chem. Phys. 115 (2009) 656–659.
[7] D. Kalaiselvi, R. Mohan Kumar, R. Jayavel, Cryst. Res. Technol. 43 (2008) 851–856.
[8] X.J. Liu, Z.Y. Wang, D. Xu, X.Q. Wang, Y.Y. Song, W.T. Yu, W.F. Guo, J. Alloys Compd. 441 (2007) 323–326.
[9] R. Perumal, K. Senthil Kumar, S. Moorthy Babu, G. Bhagavannarayana, J. Alloys Compd. 490 (2010) 342–349.
[10] K. Srinivasan, J. Cryst. Growth 311 (2008) 156–162.
[11] M.R. Suresh Kumar, H.J. Ravindra, S.M. Dharmaprakash, J. Cryst. Growth 306 (2007) 361–365.
[12] M. Lenin, G. Bhavannarayana, P. Ramasamy, Opt. Commun. 282 (2009) 1202–1206.
[13] K. Sugandhi, S. Dinakaran, M. Jose, R. Uthrakumar, A. Jeya Rejendran, G. Bhagvannarayana, V. Joseph, S. Jerome Das, Physica B: Condens. Matter 405 (2010) 3929–3935.

[14] J. Hernandez-Paredes, D. Glossman-Mitnik, O. Hernandez-Negrete, H. Esparza-Ponce, M.E. Alvarez, R. Rodriguez Mijangos, A. Duarte-Molle, J. Phys. Chem. Solids 69 (2008) 1974–1979.
[15] A. Wojciechowski, I.V. Kityk, G. Lakshminarayana, I. Fuks-Janczarek, J. Berdowski, E. Berdowska, Z. Tylczynski, Physica B: Condens. Matter 405 (2010) 2827–2830.
[16] M. Fleck, L. Bohaty, Acta. Crystallogr. C 60 (2004) m291–m295.
[17] P.M. Ushasree, R. Muralidharan, R. Jeyavel, P. Ramasamy, J. Cryst. Growth 210 (2000) 741–745.
[18] J. Nyvlt, R. Rychy, J. Gottfried, V. Wurzelova, J. Cryst. Growth 6 (1970) 151–162.
[19] K. Sankaranarayanan, P. Ramasamy, J. Cryst. Growth 280 (2005) 467–473.
[20] S. Dinakaran, S. Verma, S. Jerome Das, S. Kar, K.S. Bartwal, P.K. Gupta, Physica B: Condens. Matter 405 (2010) 1809–1812.
[21] J. Mary Linet, S. Jerome Das, Physica B: Condens. Matter 405 (2010) 3955–3959.
[22] K. Lal, G. Bhagavannarayana, J. Appl. Crystallogr. 22 (1989) 209–215.
[23] G. Bhagavannarayana, R.V. Ananthamurthy, G.C. Budakoti, B. Kumar, K.S. Bartwal, J. Appl. Crystallogr. 38 (2005) 768–771.
[24] B.W. Betterman, H. Cole, Rev. Mod. Phys. 36 (1964) 681–717.
[25] S.K. Kurtz, T.T. Perry, J. Appl. Phys. 39 (1968) 3798–3813.
[26] P.V. Raja Shekar, D. Nagaraju, V. Ganesh, K. Kishan Rao, Cryst. Res. Technol. 44 (2009) 652–656.
[27] A. Abu El-Fadl, A.S. Soltan, N.M. Shaalan, Cryst. Res. Technol. 42 (2007) 364–377.
[28] S. Mukerji, T. Kar, Cryst. Res. Technol. 34 (1999) 1323–1328.
[29] K. Sangwal, A. Klos, Cryst. Res. Technol. 40 (2005) 429–438.